WINDOWS INTO SAUROPSID AND SYNAPSID EVOLUTION
Essays in honor of Prof. Louis L. Jacobs, pp. 99–119, 2023

PALEODIVERSITY AND NICHE PARTITIONING OF CROCODYLIFORMS FROM THE WOODBINE GROUP (LATE CRETACEOUS: CENOMANIAN)

THOMAS L. ADAMS[1,*], STEPHANIE K. DRUMHELLER[2], and CHRISTOPHER R. NOTO[3]

[1]Witte Museum, San Antonio, TX, 78209, U.S.A., thomasadams@wittemuseum.org;
[2]Department of Earth and Planetary Sciences, University of Tennessee, Knoxville, Tennessee 37996, U.S.A., sdrumhel@utk.edu;
[3]Department of Biological Sciences, University of Wisconsin-Parkside, P.O. Box 2000, Kenosha, Wisconsin 53141, U.S.A., noto@uwp.edu

ABSTRACT Excavations at the mid-Cretaceous Arlington Archosaur Site (AAS) of north-central Texas has produced a diverse assemblage of terrestrial and coastal vertebrates including sharks, bony fishes, lungfish, amphibians, turtles, snakes, crocodyliforms, ornithopod and theropod dinosaurs, and mammals. Within this unique fauna, fossils of crocodyliforms remain the most common resident of this ancient ecosystem. Prior to work at AAS, the only two taxa recognized from the Woodbine Group were *Terminonaris* and *Woodbinesuchus*. Both these taxa are longirostrine pholidosaurs, occupying marginal to fully marine paleoenvironments. At the Arlington Archosaur Site, located within the upper strata of the Woodbine Group, at least five crocodyliform taxa have been identified, with the possibility of as many as six taxa, based on numerous cranial and post-cranial remains. The dominant constituent of the assemblage is represented by an ontogenetic series attributable to the large neosuchian crocodyliform *Deltasuchus motherali*. Several fragmentary cranial remains and isolated teeth are assigned to *Terminonaris* sp. *Scolomastax* represents a small-bodied and durophagus taxon that lived alongside larger, more generalized forms indicating that a broad taxonomic and ecological diversity of crocodyliforms existed in mid-Cretaceous Appalachia. Eusuchian crocodyliforms are represented by cranial material (including a second heterodont form), isolated teeth, procoelous vertebrae, and numerous osteoderms. The presence of such a diverse assortment of crocodyliforms at the Arlington Archosaur Site suggests individuals exhibiting widely disparate body plans and size ranges were occupying separate niches within a marginal marine ecosystem.

KEYWORDS Crocodyliformes, Woodbine Group, Cenomanian, Neosuchia, Late Cretaceous

INTRODUCTION

The mid-Cretaceous (Aptian to Cenomanian) of North America saw a major turnover within the dominant terrestrial clades as the Western Interior Seaway (WIS) spread, dividing the continent into two landmasses: Laramidia to the west and Appalachia to the east. However, understanding the exact timing and tempo of these faunal shifts is complicated by significant taphonomic biases. Fossil-bearing sites are comparatively rare from the mid-Cretaceous (Jacobs and Winkler, 1998; Weishampel et al., 2004; Zanno and Makovicky, 2013), and the best-known and -sampled localities are concentrated in the west (Ullmann et al., 2012; Krumenacker et al., 2016; Prieto-Márquez et al., 2016). The few Appalachian sites often contain poorly preserved isolated remains, which nevertheless provide tantalizing clues as to the communities present on the eastern landmass (Adams et al., 2017; Brownstein, 2018; Adrian et al., 2019; Noto et al., 2019; Drumheller et al., 2021; Noto et al., 2022).

Fossils from the Woodbine Group of north-central Texas, U.S.A., preserve a coastal ecosystem from the Cenomanian of Appalachia (Powell, 1968; Dodge, 1969; Kennedy and Cobban, 1990; Emerson et al., 1994; Lee, 1997; Jacobs and Winkler, 1998; Gradstein et al., 2004). Most Woodbine deposits yield poorly preserved, scattered fossils from a mixture of terrestrial, freshwater, and marine organisms (Lee, 1997; Head, 1998; Jacobs and Winkler, 1998; Adams et al., 2011). The Arlington Archosaur Site (AAS) represents an unusual outlier, a Woodbine deposit that is rich in well-preserved fossils (Adams et al., 2017; Adrian et al., 2019; Noto et al., 2019; Drumheller et al., 2021, Noto et al., 2022; 2023a). The AAS has produced a wide diversity of coastal taxa, including several new species (Adams et al., 2017; Main et al., 2011; Adrian et al., 2019; Noto et al., 2019;

*Corresponding author

Adrian et al., 2021; Adrian et al., 2023). Analyses of these groups suggests a complex biogeographic pattern was at play during the mid-Cretaceous transition in Appalachia, with more stereotypically Early and Late Cretaceous groups coexisting within this one ecosystem (Drumheller et al., 2021; Noto et al., 2022; 2023a).

Crocodyliforms are particularly common within the AAS, representing a wide range of body sizes and ecomorphotypes (Noto et al., 2012; Adams et al., 2017; Noto et al., 2019; Drumheller et al., 2021). Here we document all crocodyliforms present within the AAS and then discuss the factors leading to the high diversity of sympatric crocodyliforms present in this single ecosystem.

Anatomical Abbreviations — **ang**, angular; **anr**, angular ridge; **aps**, ascending process of the surangular; **bo**, basioccipital; **den**, dentary; **fio**, foramen intermandibularis oralis; **f**, frontal; **j**, jugal; **mx**, maxilla; **mxp**, posterior maxillary process; **na**, nasal; **oto**, otoccipital (opisthotic-exoccipital); **pal**, palatine; **par**, parietal; **pmx**, premaxilla; **po**, postorbital; **pob**, postorbital bar; **pop**, postorbital process; **q**, quadrate; **qd**, quadrate dorsal process; **sp**, splenial; **sq**, squamosal; **sur**, surangular; **sym**, mandibular symphysis.

Institutional Abbreviation — **AMNH**, The American Museum of Natural History, New York; **DMNH**, Perot Museum of Nature and Science (formerly the Dallas Museum of Natural History), Dallas, Texas, USA; **SMNH**, Royal Saskatchewan Museum (formerly the Saskatchewan Museum of Natural History), Regina; **WM**, Witte Museum, San Antonio, Texas, USA.

AGE AND GEOLOGIC SETTING

The Woodbine Group is the oldest Upper Cretaceous unit on the Gulf Coastal Plain, representing primarily terrigenous, near shore, and shallow marine depositional systems, including shelf, deltaic, and fluvial environments (Fig. 1; Hedlund 1966; Oliver, 1971; Trudel, 1994; Ambrose et al., 2009; Hentz et al., 2014). Originally called the Woodbine Formation by geologist R.T. Hill during his geological survey from Big Bend to North Texas, it is named for the town of Woodbine in Cooke County, Texas. Surface outcrops of the Woodbine Group are exposed in a narrow, irregular band, stretching from central Texas into southern Oklahoma (Dodge 1969; Johnson 1974; Oliver 1971; Trudel 1994). Two units are currently recognized based on sequence stratigraphic and biostratigraphic criteria: the lower Dexter Formation representing marginal and marine environments (Bergquist 1949; Dodge 1952; 1968; 1969; Johnson 1974; Oliver 1971) and the overlying Lewisville Formation, which represents a low-lying coastal plain (Oliver 1971; Powell 1968). In the study area the Woodbine Group sits unconformably over the Grayson Marl (Washita Group) and is separated by another unconformity from the overlying Eagle Ford Group. The Woodbine Group is separated by a period of marine deposition lasting at least ten million years from the older terrestrial units that distinguish the Lower Cretaceous Trinity Group (Winkler et al., 1995).

Sequence stratigraphic and chronostratigraphic studies suggest a maximum age of middle-early Cenomanian for the Woodbine Group (Adams and Carr 2010; Ambrose et al. 2009; Donovan et al. 2015; Vallabhaneni et al. 2016). The presence of the ammonite *Conlinoceras tarrantense*, a zonal marker for the base of the middle Cenomanian, in the Lewisville Formation provides an age estimate no younger than early middle Cenomanian (approximately 96 Ma) (Kennedy and Cobban, 1990; Emerson et al., 1994; Lee, 1997; Jacobs and Winkler, 1998; Gradstein et al., 2004). However, Ambrose et al. (2009) suggests the Lewisville Formation may be as young as late Cenomanian, with overall deposition of the Woodbine Group ending around 92 Ma.

The AAS consists of a 200 meter long, 5-meter-thick outcrop belt that includes the primary fossil quarry and isolated patches of fossiliferous exposure. Fossils are found in deposits interpreted as terrestrial, freshwater, and marine (Noto, 2015; Noto et al., 2012, 2019, 2022, 2023b; Adams et al., 2017). The main quarry contains four lithofacies (A-D) that indicate increasing marine influence through time (Noto, 2015; Adams et al., 2017). Fossils are largely concentrated in the lowermost facies (A), a dark brown, sandy siltstone that transitions upwards into a dark gray, carbonaceous sandy siltstone (Adams et al., 2017). These layers are rich in plant macrofossils, palynomorphs, invertebrates, and well-preserved but disarticulated vertebrate remains (Noto, 2015; Noto et al., 2012; Main et al., 2014; Adams et al., 2017). Facies A represents a low-energy freshwater or brackish coastal wetland proximal to the ancient coastline (Noto, 2015; Noto et al., 2012; Adams et al., 2017).

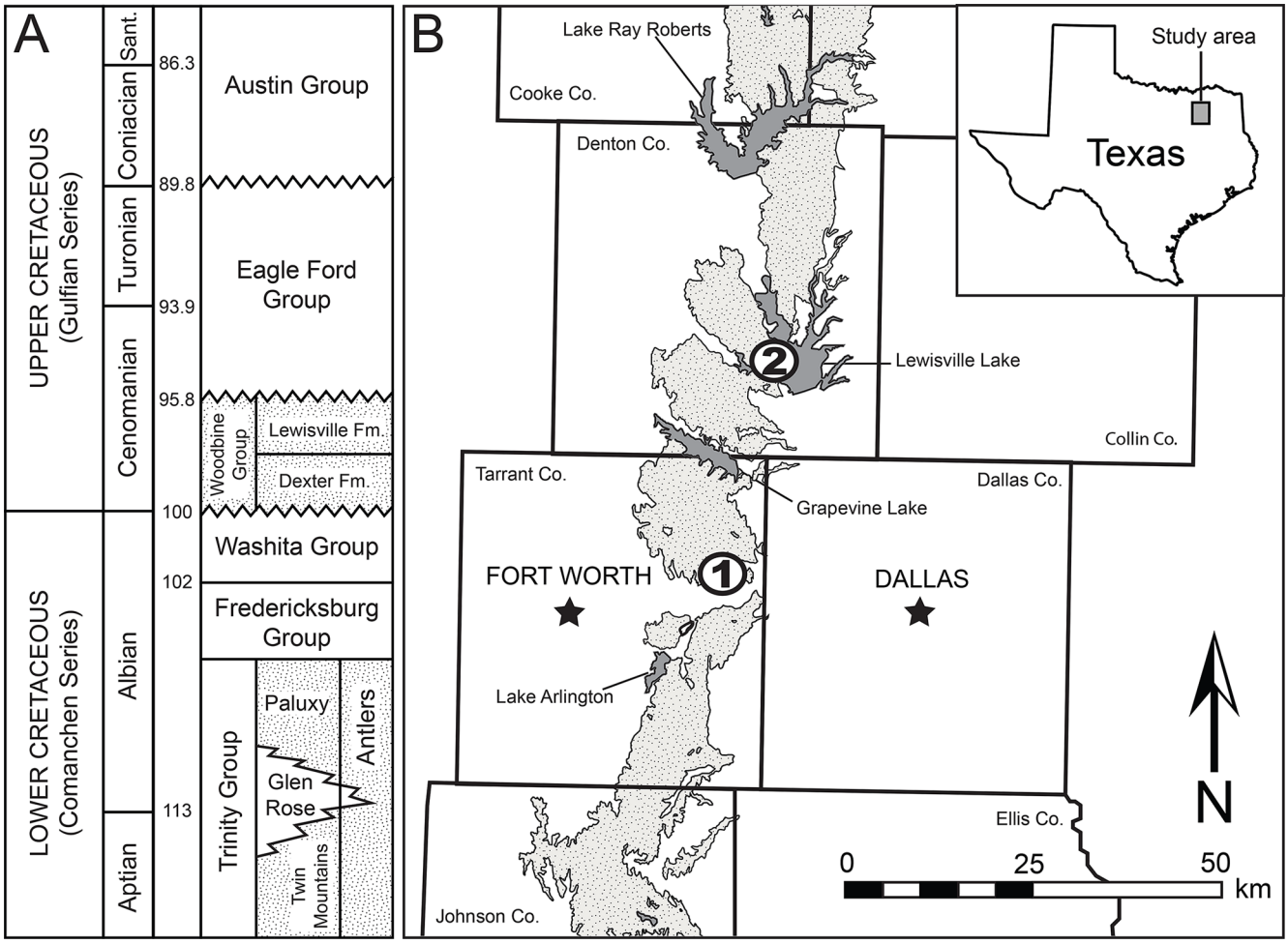

FIGURE 1. Location and geologic setting of the Arlington Archosaur Site (AAS). **A**, stratigraphic column for the Upper Cretaceous of north-central Texas showing the position of the Woodbine Group relative to timescale and adjacent geologic units. Stippled intervals represent terrestrial deposits. Time scale based on Gradstein et al. (2004). **B**, Generalized map of geologic units in the Fort Worth Basin, showing enlarged area from white box of inset map of Texas. Location of AAS, **1**; location of Lewisville Lake (*Terminonaris* localities), **2**. Modified from Barnes et al. (1972), Strganac (2015), Noto et al. (2021).

MATERIALS AND METHODS

3D Modeling — 3D digital modeling and reconstructions on numerous fossils from AAS was conducted using a variety of technologies and software. Digital scanning of individual elements was done with NextEngine™ HD Desktop 3D scanner and ScanStudio™ HD PRO software (NextEngine™, 2008) and with Revopoint™ POP 2 3D scanner and Revo Scan software (Revopoint 3D Technologies, 2014). Reconstruction and rendering of 3D models were completed using Blender 3D creation suite version 2.8 (Blender Foundation, 2002). In the case of damaged or missing elements, the 3D digital model of the opposing elements was digitally mirrored and used in skull reconstructions.

The holotype of *Scolomastax sahlsteini* (DMNH 2013-07-1256) was microCT scanned at the Microscopy and Imaging Facility in the American Museum of Natural History using a GE Phoenix v|tome|x s 240 high resolution scanner. The scan utilized a voltage of 180 kV and current of 180 mA; 1,200 images were collected at a voxel size of 0.0837 mm. Original scan files and models for this specimen are available at Morphosource.org (Project P605). CT images were post processed with 3D Slicer v 4.11 (Fedorov et al., 2012). The specimen was first segmented using the threshold function, then the paint tool was used to manually segment the individual alveoli, which were each rendered in a color according to tooth position (incisiform, caniniform, 'premolariform', molariform) with a surface smoothing factor of 0.5.

SYSTEMATIC PALEONTOLOGY AND DESCRIPTIONS

CROCODYLIFORMES Hay, 1930
MESOEUCROCODYLIA Whetstone and Whybrow, 1983
NEOSUCHIA Benton and Clark, 1988
PALUXYSUCHIDAE Drumheller et al., 2021
DELTASUCHUS Adams et al., 2017
DELTASUCHUS MOTHERALI Adams et al., 2017
(Fig. 2)

Holotype — DMNH 2013-07-0001, partial skull and mandible

Referred Material — DMNH 2013-07-1859, partial skull and mandible; DMNH 2014-06-01, partial mandible; DMNH 2013-07-0079, right dentary and maxilla; DMNH 2013-07-0297, left premaxilla, right premaxilla; DMNH 2013-07-1888, right dentary; DMNH 2013-07-0239, left dentary; DMNH 2013-07-0218, right dentary; DMNH 2013-07-1984, right dentary; DMNH 2013-07-0240, left dentary; DMNH 2013-07-0322, left dentary; DMNH 2013-07-0228, left dentary; DMNH 2013-07-0312, right dentary; DMNH 2013-07-0802, right dentary; DMNH 2013-07-0219, left maxilla; DMNH 2013-07-1404d, left prefrontal; DMNH 2013-07-0733, left quadrate; DMNH 2013-07-0084, left lacrimal; DMNH 2013-07-1871, frontal; DMNH 2013-07-1992, left and right quadratojugals, left and right quadrates; DMNH 2013-07-1993, left lacrimal; DMNH 2013-07-1994, partial right exoccipital; DMNH 2013-07-1995, right prefrontal; DMNH 2013-07-0004, left otoccipital and right surangular; DMNH 2013-07-1997, right quadrate; DMNH 2013-07-1975, right prefrontal, left jugal; DMNH 2013-07-0178, 2013-07-0164, 2013-07-0043, 2013-07-0165, 2013-06-04 teeth; SMU 76810, articulated right surangular and angular; WM 2019-15 Ga, left premaxilla; WM 2019-15 Gb, tooth.

Description

The holotype of *Deltasuchus motherali* (DMNH 2013-07-0001) includes associated, but disarticulated craniomandibular elements ascribable to a large, adult neosuchian crocodyliform with a robust, broadly triangular snout (Adams et al., 2017; Fig. 2A, B). The specimen is incomplete, including both premaxillae, maxillae, and nasals, a left postorbital, a left jugal, a right squamosal, both quadrates, a right otoccipital, the basioccipital, both ectopterygoid, and fragments of the pterygoids and dentaries. Based on a reconstructed cranial length of 800 mm, the total body length of the holotype animal is estimated at between 5.6 and 6 meters in length (Drumheller et al., 2021).

Multiple smaller-bodied individuals are also known from AAS and ascribable to *D. motherali*, based on the following combination of characters: more robust, widely-triangular snout shape; paired pseudocanines in the maxilla (m4 and m5); paired pseudocanines in the dentary (d3 and d4); ventrally directed premaxilla; posterior process of the premaxilla overlaps anterodorsal surface of the maxilla anterolaterally, then transition to a butt joint articulation posteromedially; anterior process of the frontal extends anterior to the tip of the prefrontal; frontal excluded from the orbital margin; and enlarged supratemporal fenestrae, as well as the associated bulging of the lateral margins of the maxilla which accommodate that enlarged dentition (Adams et al., 2017; Drumheller et al., 2021). The most complete specimen of these smaller individuals when articulated (DMNH 2013-07-1859) had a cranial length of 440 mm (measured from the anteriormost tip of the premaxilla, along the midline, to the posteriormost margin of the skull table), roughly half the size of the holotype (Drumheller et al., 2021; Fig. 2C, D).

Remarks

Based on a total of 14 individuals of *Deltasuchus* are recognized from AAS, ranging in size from just under 1.5 meters long to roughly 6 meters in total length; and the assemblage provides a unique ontogenetic sampling across much of the group (Drumheller et al., 2021). *Deltasuchus motherali* (DMNH 2013-07-0001) is easily differentiated from the other two large crocodyliforms known from the Woodbine Group of Texas; *Woodbinesuchus byersmauricei* (Lee, 1997) and *Terminonaris robusta* (Adams, et al. 2011). Both of these taxa are longirostrine neosuchians with tubular snouts, while *D. motherali* has a broad platyrostral rostrum.

CROCODYLIFORMES Hay, 1930
MESOEUCROCODYLIA Whetstone and Whybrow, 1983
NEOSUCHIA Benton and Clark, 1988
PARALLIGATORIDAE Konzhukova, 1954
SCOLOMASTAX Noto et al., 2019
SCOLOMASTAX SAHLSTEINI Noto et al., 2019
(Fig. 3)

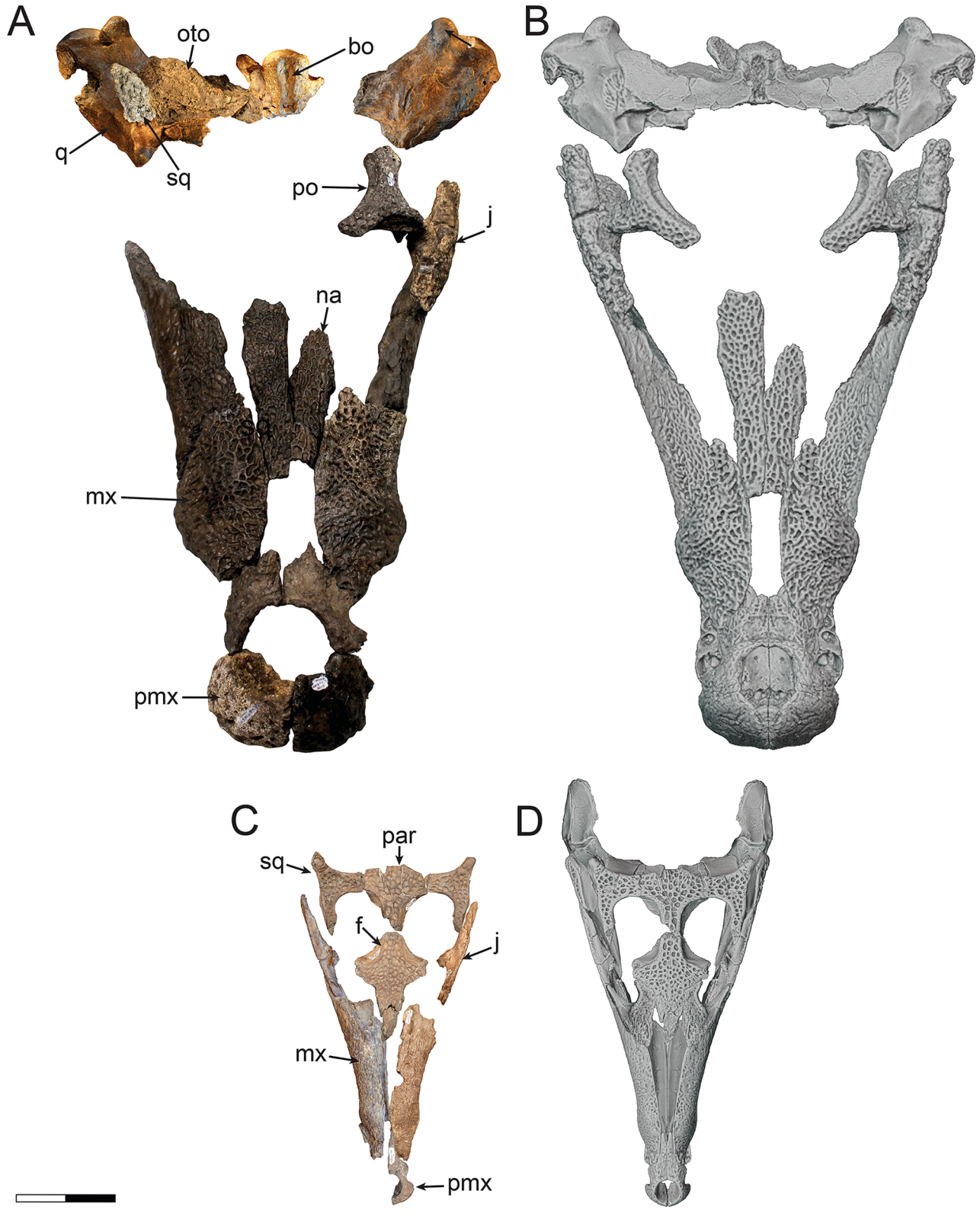

FIGURE 2. Adult skull of *Deltasuchus motherali* (DMNH 2013-07-0001; holotype), **A**, articulation of cranial elements in dorsal view; **B**, orthographic image of 3D digital reconstruction of adult skull in dorsal view. Subadult of *Deltasuchus motherali* (DMNH 2013-07-1859), **C**, cranial elements in dorsal view; **D**, orthographic image of 3D digital reconstruction of subadult skull in dorsal view. See text for anatomical abbreviations. Scale bar equals 10 cm. Modified from Adams et al. (2017) and Drumheller et al. (2021).

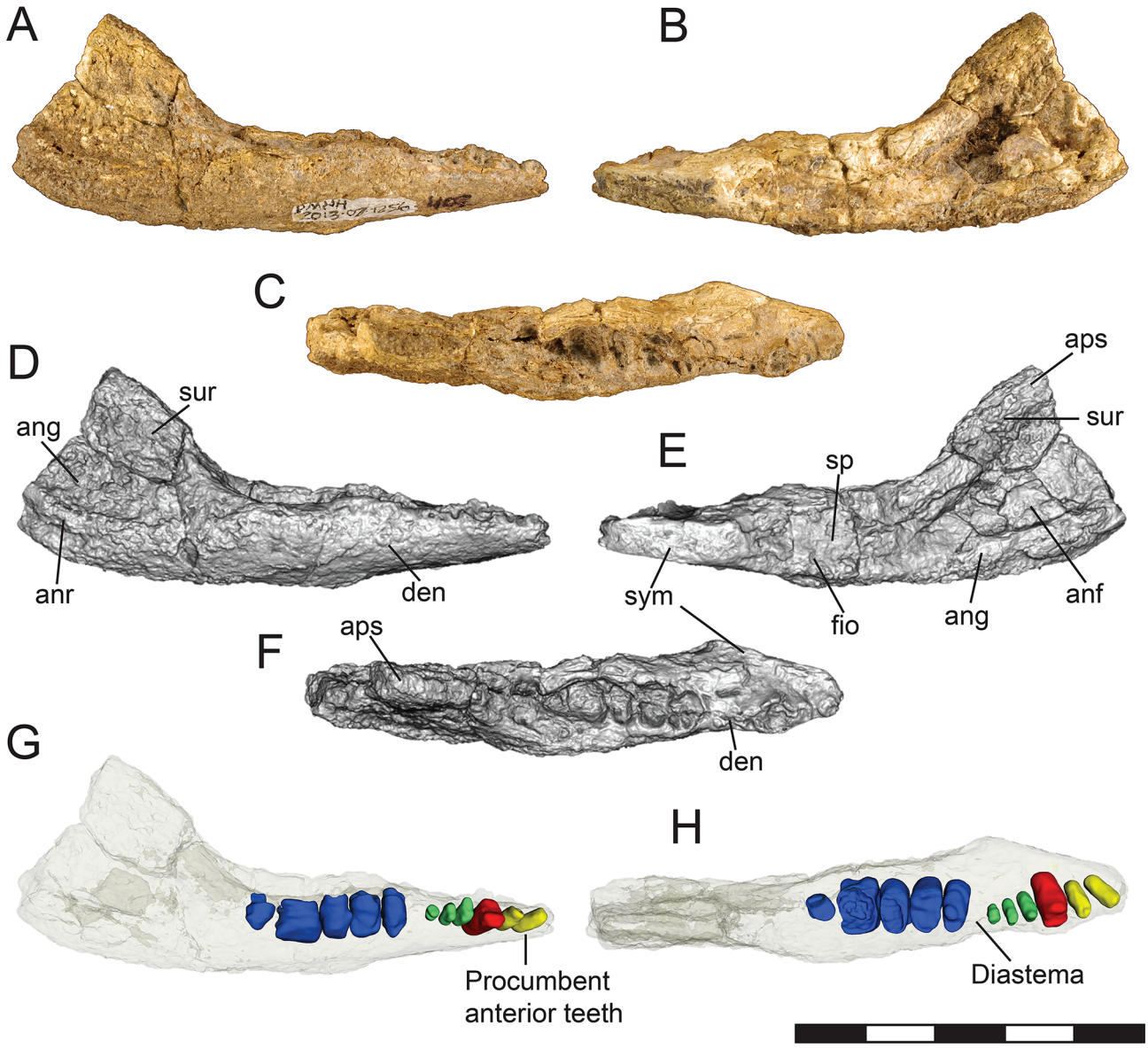

FIGURE 3. Right hemimandible of DMNH 2013-07-1256, *Scolomastax sahlsteini* in **A**, Lateral, **B**, medial, and **C**, dorsal views. CT model of DMNH 2013-07-12562 in **D**, Lateral, **E**, medial, and **F**, dorsal views. 3D Slicer images of 2013-07-12562 in **G**, Lateral and **H**, dorsal views. Incisiform in yellow, caniniform in red, 'premolariform' in green, molariform in blue. See text for anatomical abbreviations. Scale bar equals 5 cm.

Holotype — DMNH 2013-07-1256, partial right mandibular ramus.

Description

The holotype of *Scolomastax* (DMNH 2013-07-1256) is a right, lower mandible, comprising the dentary, splenial, and partial angular and surangular (Noto et al., 2019; Fig. 3A-F). Surface preservation is poor so that sutural contacts and other fine surficial details are obscured. The mandibular symphysis incorporates both the dentary and the splenial and is very elongate, extending over one-third the total length of the dentary. The dentary tapers anteriorly and expands posteriorly with two waves of prominent festooning, with associated alveolar enlargement at the third and tenth alveoli. Eleven dental alveoli are present, though none retain observable teeth. The alveoli range significantly in size, with small, procumbent alveoli in the anteriormost portion of the dentary, transitioning to significantly larger, more rectangular shaped

alveoli in the posteriormost portion of the jaw. There is a diastema between the 6th and 7th alveoli. There is no external mandibular fenestra, as the dentary is sutured to the angular and surangular. The right splenial participates in the posterior third of the mandibular symphysis. Only the anterior portion of the surangular is preserved, but what remains expands in a stepwise fashion into an unusually tall ascending, coronoid-like process. This element is mediolaterally compressed. Most of the angular is present, forming the posteroventral surface of the mandible (Noto et al., 2019).

Remarks

The partial mandible comes from a small individual and is distinguished by its low tooth count (11 alveoli; Fig. 3G-H), elongate symphysis with splenial participation, no external mandibular fenestra, a dorsally-expanded surangular forming a coronoid-like process, and an angular possessing a dorsoventral ridge. When reconstructed with the left ramus, the complete mandible would have been V-shaped in ventral view with a convex ventral margin in lateral view. The shortened toothrow and small number of enlarged posterior teeth suggests a more durophagus, or possibly omnivorous, diet. The phylogenetic position of the mandible was recovered within Paralligatoridae, although it shares characteristics with multiple mesoeucrocodylian clades (Noto et al., 2019).

CROCODYLIFORMES Hay, 1930
MESOEUCROCODYLIA Whetstone and Whybrow, 1983
NEOSUCHIA Benton and Clark, 1988
PHOLIDOSAURIDAE Zittel and Eastman, 1902
TERMINONARIS Osborn, 1904 sensu Wu et al., 2001

cf. *TERMINONARIS* sp.
(Fig. 4)

Referred Material — DMNH 2013-07-1071, left postorbital; DMNH 2013-07-1885, left postorbital; DMNH 2013-07-1868, left postorbital; DMNH 2013-07-1873, right postorbital; DMNH 2013-07-0086, right postorbital; DMNH 2013-07-0331, right postorbital; DMNH 2013-07-0225, left frontal; DMNH 2013-07-1863, parietal; DMNH 2013-07-1286, parietal; DMNH 2013-07-0049a,b, left and right squamosals; DMNH 2013-07-0168, DMNH 2013-07-0171, teeth.

Description

Terminonaris from AAS is represented by disarticulated elements found within the same bedding horizon, in close association. All elements are densely ornamented with rounded pits along the dorsal, dermal surface. The postorbitals (DMNH 2013-07-0331, DMNH 2013-07-0086, DMNH 2013-07-1071, DMNH 2013-07-1868, DMNH 2013-07-1873, DMNH 2013-07-1885; Fig. 4A-J) display a prominent anterolateral process giving a strong Y-shape to the element in dorsal view. This anterolateral process extends anterolaterally past the postorbital bar to contribute to the posteroventral border of the orbit. It projects ventrally below the level of the intertemporal bar, tapering to a point at the anteriormost projection. The projection has a smooth and shallow, concave lateral surface. The medial and posterior processes of the postorbitals form the anteromedial corner of the supratemporal fenestra. The medial process is not preserved in DMNH 2013-07-033, DMNH 2013-07-0086, DMNH 2013-07-1071, and DMNH 2013-07-1885. The descending process of the postorbital bar is smooth and short. It articulates with the ascending process of the jugal posteromedially at the dorsoventral midpoint of the postorbital bar.

The partial frontal (DMNH 2013-07-0225) is a flat element missing the anterior process that would have contacted the nasals (Fig. 4K). Only a small portion of the orbital margin is preserved. Posteriorly, the supratemporal fossa of the frontal forms the anteromedial corner of the supratemporal fenestra.

The parietals (DMNH 2013-07-1863, DMNH 2013-07-1286) are unpaired and dorsally flat elements (Fig. 4L, M). The anterior projection is very narrow, forming the dorsomedial border of the supratemporal openings. Within the supratemporal fossa, fragments of the left dorsal process of the quadrate remain in articulation on both specimens. DMNH 2013-07-1286 was exposed on the surface and has undergone weathering so that the anteriormost projection has been rounded. It does not preserve the posterior portion of the element. The posterior margin of DMNH 2013-07-1863 is broken and missing, so it is not possible to determine if the posterior margin overhangs the occiput as described by Wu et al., 2001.

Like the frontal, the squamosals (DMNH 2013-07-0049a,b) are dorsoventrally flat elements (Fig. 4N, O). In dorsal view,

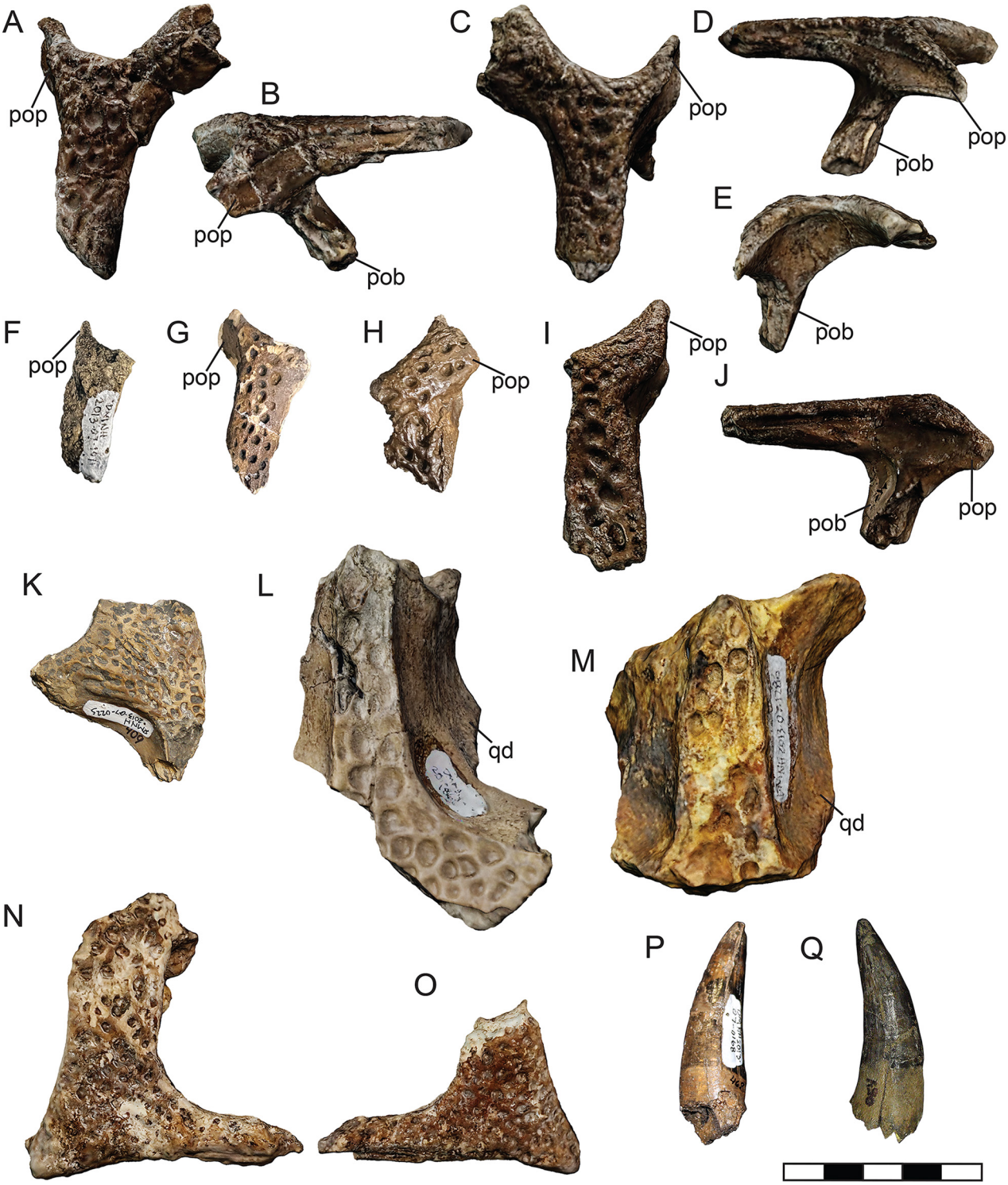

FIGURE 4. Cranial elements of cf. *Terminonaris* sp. Left postorbital DMNH 2013-07-1868 in **A**, dorsal, **B**, lateral views; right postorbital DMNH 2013-07-1873 in **C**, dorsal, **D**, lateral, and **E,** anterior views; **F**, left postorbital DMNH 2013-07-1071 in dorsal view; **G**, left postorbital DMNH 2013-07-1885 in dorsal view; **H**, right postorbital DMNH 2013-07-0331 in dorsal view; right postorbital DMNH 2013-07-0086 in **I**, dorsal, **J**, lateral views; **K**, parietal DMNH 2013-07-1286 in dorsal view; **L**, parietal DMNH 2013-07-1863 in dorsal view; **M**, left frontal DMNH 2013-07-0225 in dorsal view; **N**, **O**, left and right squamosals, DMNH 2013-07-0049a,b in dorsal view; Teeth DMNH 2013-07-0168, **P** and DMNH 2013-07-0171, **Q** labiolingual views. See text for anatomical abbreviations. Scale bar equals 5 cm.

the triangular posterolateral process extends posterolaterally beyond the level of the anterior and medial processes. Posterior to the supratemporal fenestra, the medial process is much narrower than the anterior process. In occipital view, DMNH 2013-07-0049a has a pronounced ventral projection extending from the posterolateral process. Remnants of this same projection can be seen in DMNH 2013-07-0049b.

The teeth (DMNH 2013-07-0168, DMNH 2013-07-0171) are long, slender, conical and recurved (Fig. 4P, Q; Appendix 1). The enamel is smooth, with fine, basiapical striations occurring along the surface. Smooth carina without denticles are present along the mesial and distal surfaces. The upper apical region of DMNH 2013-07-0171 has a slight sigmoidal curve but may be a result of wear at the apex. In cross-section, the teeth have a circular base.

Remarks

The presence of *Terminonaris* is well established within the middle Cenomanian (96 Ma) Woodbine Group due to multiple individuals recovered from deposits of the upper Lewisville Formation at Lewisville Lake in Denton County, Texas (Adams et al., 2011). However, the Lewisville Lake material is represented by only rostral and postcranial elements. Excluding the teeth, no direct comparison is possible with that of the AAS fossils. However, the AAS cranial material described above can be tentatively assigned to *Terminonaris* due to strong similarities to that of the type specimen (AMNH 5850) and SMNH P2411.1 of *T. robusta* (Mook, 1934; Wu et al., 2001). Specifically, the anterolaterally directed anterolateral process on the postorbital, not presence in *Deltasuchus motherali* (Adams et al., 2017). The teeth can be distinguished from the teeth of *D. motherali*, which have broader, conical crowns with closely spaced basiapical ridges that terminate shortly before the apex of the crown (Adams et al., 2017). The teeth can also be distinguished from those of *Woodbinesuchus*, which are more lingually curved, possess strong, basiapical ridges, and a subcircular to ovoid base in cross-sectional view (Lee, 1997). Postorbitals DMNH 2013-07-1868 and DMNH 2013-07-1873 most likely represent the left and right elements for a single individual. Similarly with the squamosals DMNH 2013-07-0049a and 2013-07-0049b. Based on the postorbitals, the minimum number of individual *Terminonaris* is 3, and potentially 5 when considering the size differences between them (Fig. 4A-J). This suggests another potential ontogenetic group from AAS.

CROCODYLIFORMES Hay, 1930
MESOEUCROCODYLIA Whetstone and Whybrow, 1983
NEOSUCHIA Benton and Clark, 1988
EUSUCHIA Huxley, 1875

EUSUCHIA indet.
(Fig. 5)

Referred Material — DMNH 2013-07-1066, DMNH 2013-07-2085, dentary; DMNH 2013-07-2058, DMNH 2013-07-2059, DMNH 2013-07-2060, DMNH 2013-07-2061, DMNH 2013-07-2062, teeth; DMNH 2013-07-1779, cervical vertebra; DMNH 2013-07-0537, DMNH 2013-07-0713, DMNH 2013-07-0714, DMNH 2013-07-0718, DMNH 2013-07-2064, DMNH 2013-07-2066, DMNH 2013-07-2073, dorsal vertebra; DMNH 2013-07-0056, DMNH 2013-07-0715, DMNH 2013-07-0716, DMNH 2013-07-1665, DMNH 2013-07-2068, DMNH 2013-07-2069, caudal vertebra; DMNH 2013-07-0020, DMNH 2013-07-0035, DMNH 2013-07-0037, DMNH 2013-07-1065, DMNH 2013-07-1269, DMNH 2013-07-1270, DMNH 2013-07-1271, DMNH 2013-07-1272, DMNH 2013-07-1273, DMNH 2013-07-1274, DMNH 2013-07-1276, DMNH 2013-07-1277, DMNH 2013-07-1280, DMNH 2013-07-1281, DMNH 2013-07-1283, DMNH 2013-07-1439, DMNH 2013-07-1474, DMNH 2013-07-1477, DMNH 2013-07-1509, DMNH 2013-07-1539, DMNH 2013-07-1562, DMNH 2013-07-1662, DMNH 2013-07-1946, DMNH 2013-07-2057, DMNH 2013-07-2065, DMNH 2013-07-2078, DMNH 2013-07-2079, DMNH 2013-07-2080, DMNH 2013-07-2081, DMNH 2013-07-2082, DMNH 2013-07-2083, DMNH 2013-07-2067, DMNH 2013-07-2071, DMNH 2013-07-2072, DMNH 2013-07-2074, DMNH 2013-07-2075, DMNH 2013-07-2076, DMNH 2013-07-2077, DMNH 2013-07-2086, DMNH 2013-07-2087, osteoderms.

Description

At the Arlington Archosaur Site, two partial dentaries (DMNH 2013-07-1066 and DMNH 2013-07-2085) have been recovered and assigned to Eusuchia (Fig. 5A, B; Appendix 1). DMNH 2013-07-1066 possesses alveoli positioned along the labial edge with raised margins. The alveoli are oval and separated by distinct grooves. Alveoli changes from oval to more circular in DMNH 2013-07-2085, suggesting a heterodont dentition. DMNH 2013-07-1066 preserves a single tooth that is triangular in outline in lingual/labial view and is medio-

laterally compressed. There are smooth mesial and distal carinae. A constriction separates the tooth crown from the root. The surface ornamentation consists of thin parallel longitudinal ridges that converge towards the apex on both lingual and labial surfaces.

Additionally, Five isolated teeth (DMNH 2013-07-2058, DMNH 2013-07-2059, DMNH 2013-07-2060, DMNH 2013-07-2061, DMNH 2013-07-2062) representing two distinct morphotypes have also been recovered (Fig. 5C-G). DMNH 2013-07-2060 and DMNH 2013-07-2061 are small, lanceolate teeth with a pointed apex, labio-lingually compressed, and a weak mesiodistal constriction at the base of the crown. They have smooth carinae and weak basiapical striations. The second morphotype (DMNH 2013-07-2058, DMNH 2013-07-2059, DMNH 2013-07-2062) is also lanceolate, but shorter with a more rounded apex. It is also labio-lingually compressed, with distinct carinae, weak basiapical striations, and a constricted base.

Fourteen isolated procoelous vertebrae have been recovered from AAS, of which 10 are isolated centra, disassociated from their neural arches (Appendix 1). All possess a cup-shaped anterior cotyle and a low, rounded condyle surrounded by a smooth shelf posteriorly. DMNH 2013-07-1779 represents the only cervical vertebra recovered, thus far (Fig. 5H). The centrum is unfused to the neural arch. It represents a more posterior cervical, due to the position of the diapophysial and parapophysial processes, and the lack of a hypapophysial process. The anterior and posterior articular surfaces of the centrum are circular and roughly equal in height and width. In lateral view, the centrum is spool-shaped and is smooth along the ventral surface. The parapophyses are situated dorsoventrally at the centrum's anterior margin. The diapophyses project laterally along the length of the dorsolateral margin of the centrum.

DMNH 2013-07-2066 is an anterior dorsal vertebra unfused from its neural arch (Fig. 5I). In posterior view, the articular surface of the centrum is wider, extending laterally beyond the centrum's anterior margin. In lateral view, the centrum is spool-shaped, and the wall of the centrum is concave. A deep hypapophysial process and keeled ridge extend anteroposteriorly along the ventral surface. DMNH 2013-07-0718 and DMNH 2013-07-1665 are also anterior dorsal vertebrae unfused from their neural arches. There is no indication of a hypapophysial process, but the lateral surface of the centra are concave giving a pinched shape to the ventral surface. DMNH 2013-07-0537 is a mid-dorsal vertebra which includes a centrum and associated, unfused neural arch. The centrum is anteroposteriorly long, being nearly twice as long as high. The neurocentral sutures are rugose and extend the length of the centra. There is no indication of a hypapophysial processes or keels on the ventral surface. The unfused neural arch is nearly complete, missing the prezygapophyses and portions of the neural spine. The transverse processes are located on the neural arch at the level of the neural canal. The neural canal is large, similar in size to the anterior articular surface of the centrum. Its shape is sub-circular, being wider dorsally at the position of the transverse processes. DMNH 2013-07-0713 (Fig. 5J), DMNH 2013-07-0714, DMNH 2013-07-2064, and DMNH 2013-07-2073 represent more posterior dorsal vertebrae. Much like DMNH 2013-07-0537, they are anteroposteriorly twice as long as high. DMNH 2013-07-0714 is the only one to have had a fused neural arch but is broken at the dorsal surface of the centrum.

DMNH 2013-07-0715 is a more proximal caudal vertebra (Fig. 5K). The base of the transverse process extends halfway along the anteroposterior length of the centrum. Although the neural arch is not preserved, the rough, broken dorsal surface indicates that the neural arch was fused to the centrum. The anterior and posterior articular surfaces are circular and roughly equal in shape and size. DMNH 2013-07-0716, DMNH 2013-07-2068, and DMNH 2013-07-2069 are mid-caudal vertebra with elongated centra in lateral view with fused neural arches, although much of the neural spine are missing for DMNH 2013-07-2068 and DMNH 2013-07-2069 (Fig. 5L, M). The articular facets of the prezygapophyses are positioned lower than that of the postzygapophyses. The base of the neural arch for DMNH 2013-07-0716 extends along the anteroposterior length of the centrum.

Forty isolated osteoderms have been collected from the AAS, 38 of which can be classified into four general morphotypes; 15 belonging to morphotype 1, 13 to morphotype 2, 8 to morphotype 3, and 2 to morphotype 4 (Fig. 5N-Z; Appendix 1).

Morphotype 1 — these osteoderms are rectangular to subrectangular in shape, being longer anteroposteriorly than they are mediolaterally wide (Fig. 5N-P). Their average width-to-length ratio is approximately 0.78. They are devoid of a dorsal keel or an anterolateral process. Dorsally, they exhibit a well-defined, convex articular facet, representing

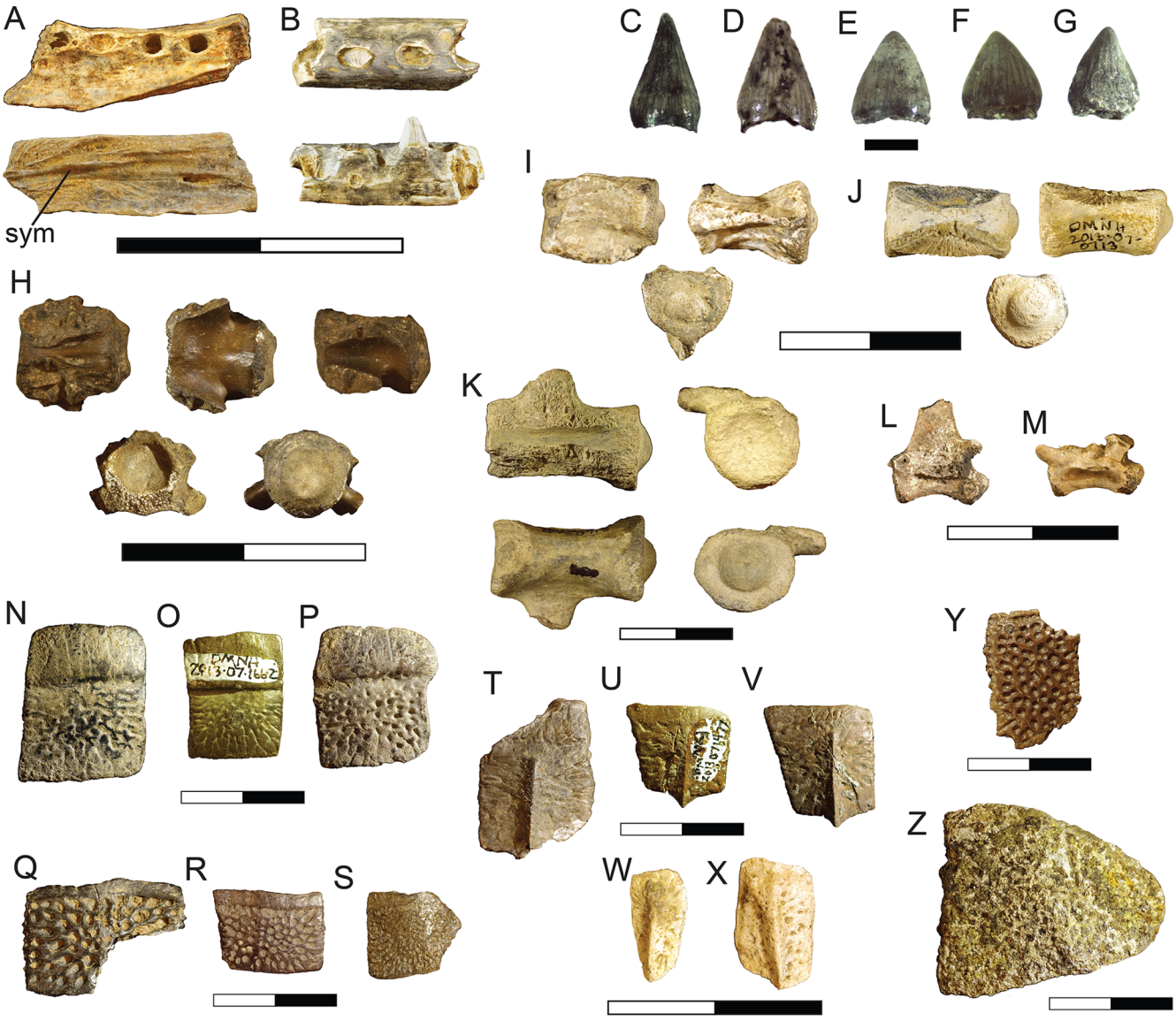

FIGURE 5. Isolated cranial and postcranial elements of Eusuchia indet. Dentary DMNH 2013-07-2085, **A**, in dorsal and medial views; dentary DMNH 2013-07-1066, **B**, in dorsal and medial views; teeth **C**, DMNH 2013-07-2061, **D**, DMNH 2013-07-2060, **E**, DMNH 2013-07-2058, **F**, DMNH 2013-07-2062, and **G**, DMNH 2013-07-2059, in mesial or distal views; cervical vertebra DMNH 2013-07-1779, **H**, in dorsal, ventral, lateral, anterior, and posterior views; dorsal vertebra DMNH 2013-07-2066, **I**, in lateral, ventral, and posterior views; dorsal vertebra DMNH 2013-07-0713, **J**, in dorsal, lateral, and posterior views; caudal vertebra DMNH 2013-07-0715, **K**, in dorsal, anterior, ventral, and posterior views; caudal vertebra DMNH 2013-07-0716, **L**, and DMNH 2013-07-2068, **M**, in lateral views; morphotype 1 osteoderms, DMNH 2013-07-1274, **N**, DMNH 2013-07-1662, **O**, DMNH 2013-07-1273, **P**, in dorsal views; morphotype 2 osteoderms, DMNH 2013-07-0035, **Q**, DMNH 2013-07-2076, **R**, DMNH 2013-07-2077, **S**, in dorsal views; morphotype 3 osteoderms, DMNH 2013-07-0020, **T**, DMNH 2013-07-1477, **U**, DMNH 2013-07-2067, **V**, in dorsal views; morphotype 4 osteoderms, DMNH 2013-07-1065, **W**, DMNH 2013-07-2071, **X**, in dorsal views; osteoderm DMNH 2013-07-0037, **Y**, in dorsal view; osteoderm DMNH 2013-07-1562, **Z**, in dorsal view. See text for anatomical abbreviations. Scale bar for **C-G** equals 1 mm, all others equal 2 cm.

approximately 40% of the anteroposterior length. This suggests a deep, imbricating articulation to the posterior edge of the next anterior osteoderm. The dorsal surface is ornamented by small, shallow pits or grooves. The ventral surface is smooth with small neurovascular foramina across the ventral surface. These are the most common of the eusuchian osteoderms from AAS and correspond to more medial, paravertebral osteoderms of the dermal shield (Hill, 2010).

Morphotype 2 — like morphotype 1, these are rectangular to subrectangular in shape, but are mediolaterally wider than the anteroposterior length (Fig. 5Q-S). The average width-to-length ratio is approximately 1.25. DMNH 2013-07-2065 and DMNH 2013-07-2074 demonstrate very shallow keels down the midline, while all others show no indication of a dorsal keel or anterolateral process. They have a smooth, narrow anterior margin for an imbricating articulation with the next anterior osteoderm. The dorsal surface is ornamented with deep, circular pits. DMNH 2013-07-2077 is strongly concave, giving the osteoderm a nearly 100^{o} bend in axial view. Similar to morphotype 1, the ventral surface is smooth with neurovascular foramina. Like morphotype 1, these characterize paravertebral osteoderms with DMNH 2013-07-2077 positioned at the most-lateral boundary along the dermal shield (Hill, 2010).

Morphotype 3 — these are subrectangular being longer anteroposteriorly than they are mediolaterally wide (Fig. 5T-V). They bear a slightly offset, parasagittally oriented keel. The keels are relatively low and extend posteriorly beyond the posterior osteoderm margin to form a distinct point. Much like morphotype 2, they also have a narrow anterior margin. In axial view, they are concave. The ventral surface is also smooth. Morphotype 3 best represents more laterally positioned dorsal, accessory osteoderm, appendicular osteoderms, or possibly caudal osteoderms (Hill, 2010).

Morphotype 4 — DMNH 2013-07-1065 and DMNH 2013-07-2071 are oval to subrectangular in shape with an obliquely oriented midline keel (Fig. 5W, X). There is no indication of an anterior margin for articulation with the next anterior osteoderm. They are most similar to morphotype 3 in also being concave. These represent the smallest identified osteoderms yet found in the AAS and are most likely appendicular osteoderms associated with the limbs (Hill, 2010).

DMNH 2013-07-0037 does not fit into any of the four morphotypes described above. It is rectangular in shape, being longer anteroposteriorly than they are mediolaterally wide (Fig. 5Y). However, it differs from the morphotype 1 in that it has a very narrow and slightly upturned, anterior articular margin. It is dorsoventrally flat and plate-like, with its dorsal surface ornamented with deep, circular pits. The left and right margins possess sutural articulation for the osteoderm directly medial and lateral to it. Its position along the osteodermal shield is unknown.

DMNH 2013-07-1562 also differs from the others significantly (Fig. 5Z). It has undergone surface exposure and weathering, so that surface ornamentation and the presence of an articular margin is difficult to discern. It is D-shaped in dorsal view, with a broken, straight medial border and a convex lateral margin. An obliquely oriented keel trends laterally to the posterior border. It is strongly concave in axial view. DMNH 2013-07-1562 corresponds to a nuchal osteoderm (Hill, 2010).

Remarks

Outside of *Deltasuchus motherali*, numerous small, isolated elements assigned to Eusuchia are among some of the most common elements recovered from the AAS assemblage. Both dentaries described above differ from *Scolomastax* (DMNH 2013-07-1256) in the shape and position of alveoli, symphyseal morphology, and parallel margins (Noto et al., 2019). The five isolated teeth demonstrate an atoposaurid-like dentition with lanceolate shaped teeth characteristic of taxa similar to *Theriosuchus pusillus* Owen, 1879. The dentaries and teeth are consistent with taxa such as *Theriosuchus* and *Wannchampsus* (Adams, 2014), suggesting this material may belong to a basal eusuchian, marking the presence of another taxon of small-bodied, heterodont crocodyliform in the Woodbine Formation.

Procoelous vertebrae, in which the anterior end is concave, and the posterior end is convex, are characteristic of members of Eusuchia. Neurocentral fusion occurs in a predictable pattern across crocodyliforms, with neonates exhibiting a lack of fusion along their entire vertebral column and sutural fusion progressing from caudal to cranial elements, with complete fusion of the cervical vertebrae used as an indicator of skeletal maturity (Brochu, 1996). The lack of fusion exhibited in most AAS eusuchian vertebrae suggests that these specimens were all immature individuals.

The osteoderms are identified as belonging to Eusuchia based on the following characteristics: small and rectangular to semi-rectangular in outline; keeled; imbricating leading edge; lacking the anterolateral process as seen in non-eusuchian neosuchians, such as goniopholidids and pholidosaurids.

CROCODYLIFORMES Hay, 1930

CROCODYLIFORMES indet.

(Fig. 6)

Referred Material — DMNH 2013-07-0018, left maxilla and palate

Description

DMNH 2013-07-0018 is a nearly complete left maxillae and palate (Fig 6; Appendix 1). Preservation quality is poor due to heavy gypsum invasion and weathering of the skull. As a result, neurovascular foramina and surface texture are not clearly visible. Even with the poor surface preservation, there is no indication of deep pitting or a strongly rugose surface texture. The maxilla is crushed dorsoventrally, and the posterior maxillary process and palate are fused and separated from the main body of the maxilla. In dorsal view, the lateral border of the maxilla is medially curved anteriorly and becomes straighter posteriorly (Fig 6A, C). There is a slight bulge at the level of the third maxillary tooth. The premaxilla-maxilla suture is obliquely oriented. The maxilla has edge-to-edge contact with the nasal along its straight dorsomedial margin. Posteriorly to this, the medial margin trends obliquely away from the midline. The secondary palate is well preserved with crushing of the palatal shelves medial to the alveolar margin. The palate is fused to the maxilla in the posteriorly extended secondary palate (Fig 6B, D). It extends posteriorly between the suborbital fenestrae, forming a narrow palatine bar with a straight lateral margin. The palatine bar is part of the medial border of the suborbital fenestra, with the posterior maxillary process forming the lateral border.

Eight tooth positions are present in the maxilla, with 5 teeth preserved in situ (Fig. 6B; Appendix 1). The alveoli increase in size from the first alveolus to the third, which is the largest in the maxilla and results in a slight lateral bulge in the maxillary margin. Four alveoli are preserved in the posterior maxillary process, with only one tooth in situ (Fig. 6D). The alveoli again decrease in size after the third. The posterior- most alveoli are not well preserved due to transverse crushing. The gap between the maxilla and the posterior maxillary process is indeterminate, so the total number of tooth positions for this taxon is unknown. The teeth are poorly preserved and have conical-shaped crowns with no indication of carinae or striations.

Remarks

Despite the poor preservation, reconstructing the rostrum of DMNH 2013-07-0018 suggests it was platyrostral in shape. It can be distinguished from *Deltasuchus motherali* whose maxilla tapers anteriorly to a narrow rostral constriction that is slightly upturned dorsally (Adams et al., 2017; Drumheller et al., 2021; Fig. 7). DMNH 2013-07-0018 also does not share the paired pseudocanines in the maxilla (m4 and m5) that help diagnose *D. motherali*. It is also discernable from the longirostrine taxa *Woodbinesuchus* and *Terminonaris* with their tubular snouts. Unlike *Scolomastax*, the teeth of DMNH 2013-07-0018 suggest a homodont dentition (Noto et al., 2019). The presence of an enlarged third maxillary tooth is a feature shared with *Wannchampsus kirpachi* from the Early Cretaceous of Texas and with the clade Paralligatoridae (Adams 2014).

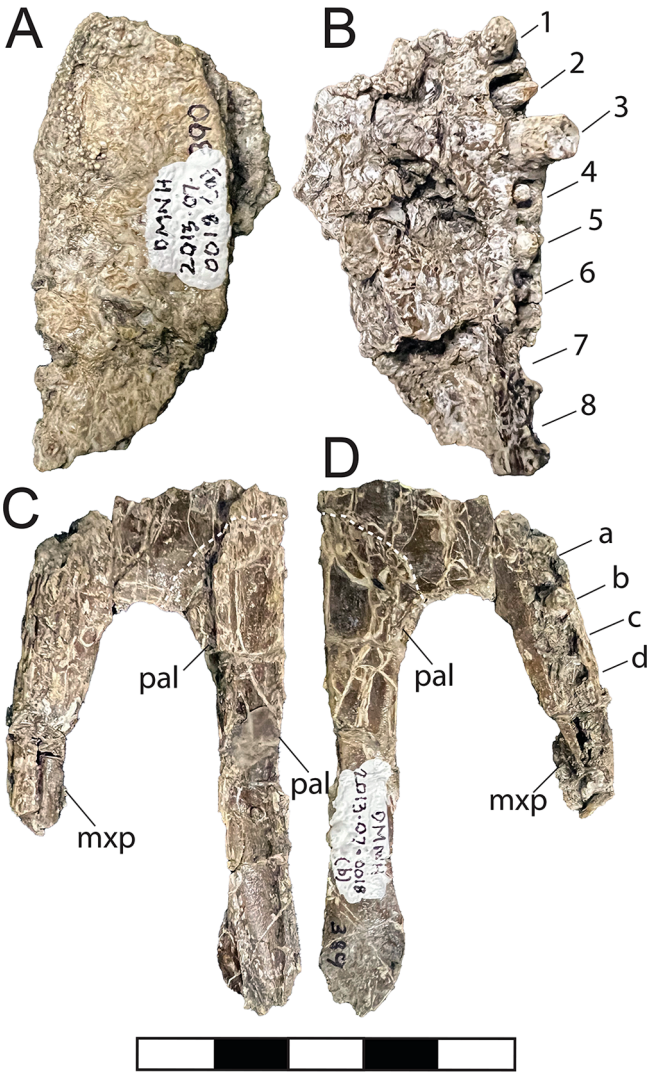

FIGURE 6. Left maxilla and palate of Crocodyliformes indet. DMNH 2013-07-0018 in dorsal, **A** and **C**, and ventral **B** and **D**, views. See text for anatomical abbreviations. Scale bar equals 5 cm.

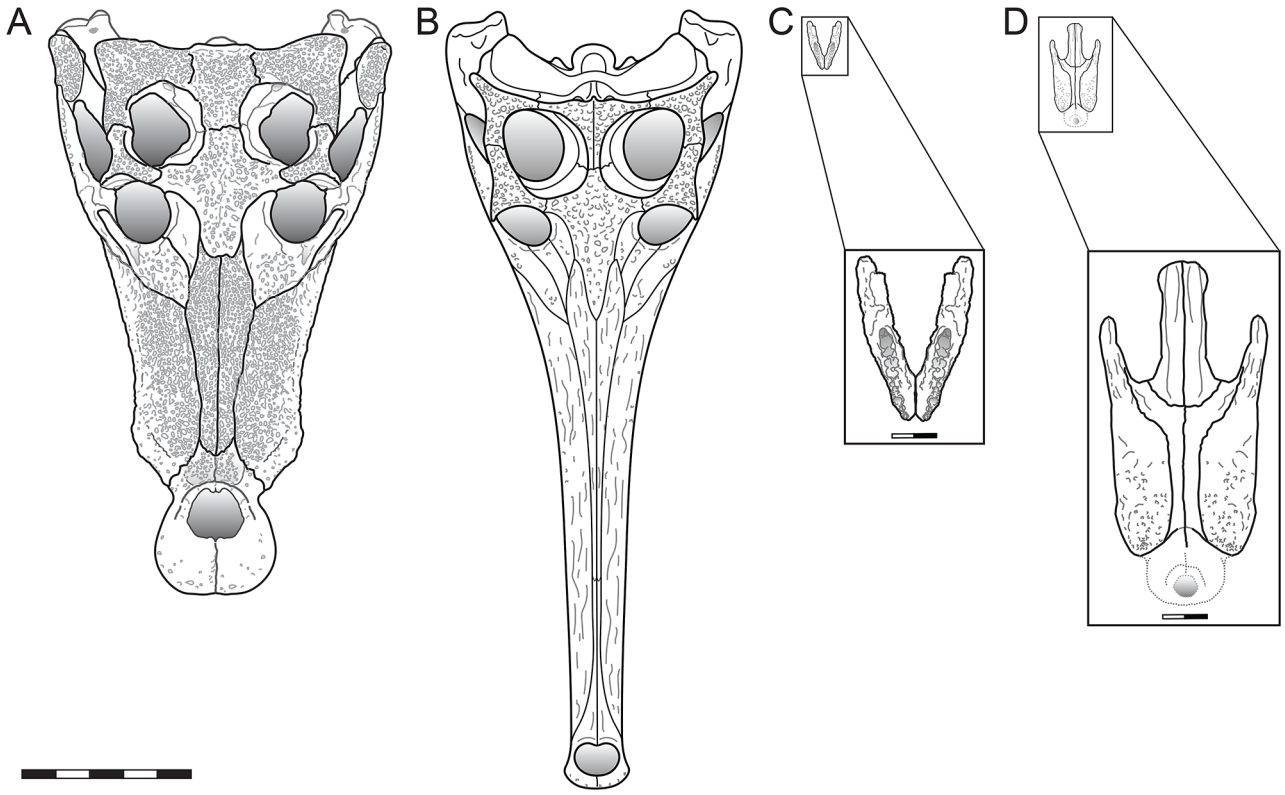

FIGURE 7. Comparisons of identifiable AAS Crocodyliformes. **A**, reconstruction of the skull of *Deltasuchus motherali*, modified after Adams et al. (2017); **B**, reconstruction of the skull of *Terminonaris robusta*, modified after Wu et al. (2001); **C**, reconstruction of the lower jaw of *Scolomastax sahlsteini*, modified after Noto et al. (2019); **D**, reconstruction of maxilla and palate of Crocodyliformes indet. (DMNH 2013-07-0018) Scale bar equals 50 cm. Scale bar in the inset boxes equals 2 cm.

DISCUSSION

Extant, sympatric crocodylians ecologically partition their habitats to reduce direct competition for resources (Drumheller and Wilberg, 2020). This often takes the form of dietary niche partitioning, which is itself reflected in variation of maximum body size, snout shape (Brochu, 2001; Drumheller and Wilberg, 2020), and dental morphologies (D'Amore et al., 2019). While modern crocodylian diversity within any single habitat rarely exceeds two or three sympatric species (Brochu, 2001), fossil assemblages across crocodyliformes can reach as high as seven morphologically and ecologically distinct species (Salas-Gismondi et al., 2015). This increased intra-site diversity is often seen during high stands in global crocodyliform diversity (Markwick, 1998a), often driven by a combination of favorable climatic conditions (Markwick, 1998b) and ecomorphological niche occupation well outstripping that seen in the present day (Brochu, 2001; Drumheller and Wilberg, 2020).

However, these patterns of dietary niche occupation among crocodyliforms often focus on only the adult morphotypes, with less attention given to juveniles (Drumheller et al., 2021), despite the fact that extreme changes in body size and corresponding shifts in snout shape and dietary preferences are observed among extant members of the clade (e.g. McIlhenny, 1935; Ross and Magnusson, 1989; Gignac and O'Brien, 2016; Gignac et al., 2019).

The AAS supported at least five crocodyliform taxa, and possibly as many as six (Fig. 7). These groups exhibit a range in snout shapes and body sizes, suggesting dietary partitioning is driving this high diversity (Adams et al., 2017; Noto et al., 2019; Drumheller et al., 2021) Additionally, these groups are often represented by multiple individuals sampling much of their ontogenetic variation, especially *Deltasuchus* (Drumheller et al., 2021) and *Terminonaris*. Partnered with the low transport seen in the fossil assemblage (Adams et al., 2017; Noto et al., 2019; Drumheller et al., 2021), this suggests that juveniles and adults were not separating out geographically

but were instead living and dying in the same area. This means that potential dietary competition and niche partitioning must be addressed across the full range of these groups' body sizes (Drumheller et al., 2021).

By far, the most common crocodyliform present in the AAS ecosystem was *Deltasuchus*. As adults, members of these groups had a broadly triangular snout with sturdy, conical teeth, morphologies which are consistent with a generalist feeding strategy (D'Amore et al., 2019; Drumheller and Wilberg, 2020; Fig 2A, D and Fig. 7A). This interpretation is further bolstered by the presence of bite marks attributable to *Deltasuchus* on smaller turtles ranging through subadult dinosaurs (Noto et al., 2012). However, the youngest and correspondingly smallest individuals known from this clade had comparatively slender dentition and narrower snouts, which pushes them more into an ecomorphotype consistent with targeting smaller, more compliant prey (Gignac and O'Brien, 2016; Drumheller and Wilberg, 2020; Drumheller et al., 2021 (Fig. 2C, D). This aligns with ecological observations among modern, generalist groups, in which juveniles often target small invertebrates, fish, and amphibians, while adults diverge into larger-bodies, more durable prey types (e.g., McIlhenny, 1935; Ross and Magnusson, 1989).

However, as slender as the snouts of these juvenile *Deltasuchus* were relative to adult members of their species, they never reached a degree of snout-elongation and narrowing comparable to *Terminonaris* (Adams et al., 2011; Fig 2C, D and Fig. 7B). This ecomorphotype is correlated with a preference for smaller-bodied, more compliant prey across ontogeny, even among very large-bodied individuals (Drumheller and Wilberg, 2020), which aligns with the slender dentition also seem in members of both clades (D'Amore et al., 2019). The overlap in this morphotype between relatively large-bodied species suggests significant competition might have been an issue, but the more longirostrine *Terminonaris* tends to be found in more coastal, marine environments (Jouve and Jalil, 2020; Jouve et al., 2021). Given that the AAS itself was deposited in a coastal system, the assemblage includes freshwater, brackish, marine, and terrestrial input associated with small-scale fluctuations in sea level throughout the facies present in the site (Adams et al., 2017; Noto et al., 2023b). This suggests that actual interactions between members of these species might have been minimal, given their differing salinity preferences, and both would have been ecomorphologically distinct from the similarly large-bodied, but generalist *Deltasuchus*.

Scolomastax represents a third major ecomorph in the AAS, a small-bodied taxon with strongly heterodont dentition (Noto et al., 2019; Fig 3 and Fig. 7C). This combination of snout and tooth shape is correlated with preferential consumption of harder food items, i.e. durophagy (Drumheller and Wilberg, 2020). Partnered with the deep, short snout, it is likely that this species was omnivorous or even herbivorous, especially if the short-crowned, button-shaped teeth observed in other Woodbine localities turn out to be associated with this taxon (Noto et al., 2019). Additional eusuchian dentaries differ in overall shape and tooth positioning to suggest a second morphotype of small, heterodont crocodyliforms was also present in the AAS. However, these elements are highly fragmentary, inhibiting more detailed analysis of phylogenetic relationships or ecomorphological classifications.

A fifth ecomorphotype is present at the site, but again, the identity of the species (DMNH 2013-07-0018) is not straightforward. It includes a small maxilla, palatine, and in situ dentition. The snout is blunter and more U-shaped in profile than *Deltasuchus*, potentially suggesting a more macro-generalist or durophagous ecomorphotype (Drumheller and Wilberg, 2020; Fig. 6 and 7D). The specimen also lacks the enlarged, paired pseudocanines seen in *Deltasuchus*, and instead has more conical dentition along the entire toothrow. It lacks the rostral shortening and low, anvil-shaped dentition seen in more hard-prey specialists (D'Amore et al., 2019), excluding obligate durophagy or other evidence of dietary specialization. Taken together, this indicates that this animal was some kind of macro-generalist, meaning that it was able to take prey items as big or even bigger than itself (Drumheller and Wilberg, 2020). Unfortunately, the specimen is also poorly preserved, with extensive crushing and flattening obscuring other, more diagnostic characteristics. We are unable to identify it beyond the level of Crocodyliformes, nor are we able to meaningfully comment on the ontogenetic stage this animal represents. However, we can say that it represents the only crocodyliform with this particular ecomorphotype in the Woodbine Group.

The remaining crocodyliform material from the AAS is even more ambiguous. The disassociated teeth, vertebrae, and osteoderms attributable to Eusuchia may represent elements from *Scolomastax*, the only eusuchian currently known from the site, or they might represent evidence of one or more unidentified eusuchian taxa, such as that represented by the

partial dentaries. More complete material is required to make this determination.

Woodbinesuchus byersmauricei Lee, 1997 has tentatively been identified within the AAS assemblage based on isolated teeth (Noto et al., 2019). Further investigation has shown that there is significant overlap between subadult *Deltasuchus* teeth described by Drumheller et al. (2021) and those described for *Woodbinesuchus* by Lee (1997). The holotype (SMU 74626) of *Woodbinesuchus* was recovered from the lower Dexter Formation (formerly Rush Creek Member). Its presence in the upper Lewisville Formation would extend the range of this taxa through the Woodbine Group. Currently, *Woodbinesuchus* is only known from lower jaw and postcrania (Lee, 1997). It is possible that some of the disarticulated cranial material described from AAS in this study could come from this clade. Again, without more complete material, it is impossible to determine which elements might be related to *Woodbinesuchus* and whether any of them instead represent other poorly known or even wholly unknown taxa.

Taking a broader perspective, the crocodyliform material from the AAS described here supports the record of faunal turnover and large-scale continental interchange through the 'mid' Cretaceous interval. This record supports hypotheses of widespread mid-Mesozoic cosmopolitanism and lower biodiversity that gave way to increased endemism and diversification during the Cretaceous (Zanno & Makovicky, 2011; Suarez et al., 2021; Buscalioni et al., 2011; Montefeltro et al., 2013; Turner, 2004). While this pattern is reciprocated in Woodbine Group crocodyliforms, it differs from other vertebrate groups in a few key respects. First, the named taxa *Deltasuchus*, *Scolomastax*, and *Terminonaris* are all members of lineages with distributions across Gondwana and/or Laurasia; part of the dominant, cosmopolitan fauna that persisted through the Early Cretaceous. Second, these lineages appeared to respond differentially during the transition. For example, the Paluxysuchidae, which includes *Deltasuchus* and *Paluxysuchus*, began to diverge from other neosuchians to form an endemic crocodyliform assemblage at the beginning of the Early Cretaceous, prior to many other vertebrate groups, implying the transition from Early to Late Cretaceous may have been more gradual for at least some crocodyliform clades (Drumheller et al., 2021). On the other hand, current phylogenetic analysis finds the sister taxa of *Scolomastax* in Asia, which suggests a more recent (and short-term) biogeographic connection with southern Appalachia, requiring significant interchange between these distant and periodically isolated areas in the Aptian-Albian or early Cenomanian prior to completion of the Western Interior Seaway (Noto et al., 2022). Third, members of these formerly cosmopolitan groups, a few endemic clades, and more recent immigrants combined to form a distinctive local fauna on the southwestern coast of Appalachia. The extraordinary diversity observed in the AAS and throughout Woodbine exposures was likely supported by the paleoenvironmental heterogeneity of the vast and complex coastal, delta plain, and shallow shelf ecosystems (Noto et al., 2022; 2023b). The Woodbine Group fossil assemblage represents an early stage of the transition during the emergence of later Late Cretaceous faunal assemblages, as 'mid' Cretaceous ecosystems evolved in response to major faunal interchange, sea level, and climate change, creating unique communities that in turn enhanced taxonomic diversity and endemism.

ACKNOWLEDGMENTS

We dedicate this paper to Dr. Louis L. Jacobs in recognition of his support and guidance, as a teacher, mentor, and colleague, which has been a great source of inspiration for so many. We thank the Huffines family and R. Kimball of Johnson Development, who provided access to the property on which the AAS is situated. A. Sahlstein, P. Kirchoff, and B. Walker first discovered the site, and a dedicated team of volunteers helped excavate and prepare much of the material over the past ten years. Thanks to the Perot Museum of Nature and Science, Southern Methodist University, and the Witte Museum for access to research collections. We thank H. Maddox for her assistance in production of orthographic models. We thank A. R. Fiorillo and A. K. Hastings for their valuable comments that helped improve this manuscript. This study was supported by funding from the National Geographic Society Conservation Trust grant #C325-16 to C. Noto, National Science Foundation DUE-IUSE GP-IMPACT grant #1600376 to L. McKay and S. Horn, as well as our contributors on Experiment.com.

LITERATURE CITED

Adams, R. L. & Carr, J. P. (2010). Regional depositional systems of the Woodbine, Eagle Ford, and Tuscaloosa of the U.S. Gulf Coast. *Gulf Coast Association of Geological Societies Transactions*, 60, 3–27.

Adams T. L. (2014). Small crocodyliform from the Lower Cretaceous

(Late Aptian) of Central Texas and its systematic relationship to the evolution of Eusuchia. *Journal of Paleontology*, 88, 1031–1049.

Adams, T. L., Noto, C. R., & Drumheller, S. K. (2017). A large neosuchian crocodyliform from the Upper Cretaceous (Cenomanian) Woodbine Formation of North Texas. *Journal of Vertebrate Paleontology*, 37(4), e1349776.

Adams, T. L., Polcyn, M. J., Mateus, O., Winkler, D. A., & Jacobs, L. L. (2011). First occurrence of the long-snouted crocodyliform *Terminonaris* (Pholidosauridae) from the Woodbine Formation (Cenomanian) of Texas. *Journal of Vertebrate Paleontology*, 31, 712–716.

Adrian, B., Smith, H. F., Noto, C. R., & Grossman, A. (2019). A new baenid,"*Trinitichelys*" maini sp. nov., and other fossil turtles from the Upper Cretaceous Arlington Archosaur Site (Woodbine Formation, Cenomanian), Texas, USA. *Palaeontologia Electronica*, 22, 1–29.

Adrian, B., Smith, H. F., Noto, C. R., & Grossman A. (2021). An early bothremydid from the Arlington Archosaur Site of Texas. *Scientific Reports*, 11, 9555. 10.1038/s41598-021-88905-1

Adrian, B., Smith, H., & Noto, C. R. (2023). A revision of "*Trinitichelys*" *maini* (Testudines: Baenidae) and additional material of its new genus from the Lewisville Formation (Woodbine Group, Cenomanian), Texas, USA. *Palaeontologia Electronica*, 26(2), a28. https://doi.org/10.26879/1266

Ambrose, W. A.,Hentz, T. F., Bonnaffe, F., Loucks, R. G., Brown Jr, L. F., Wang, F. P., & Potter, E. C. (2009). Sequence-stratigraphic controls on complex reservoir architecture of highstand fluvial-dominated deltaic and lowstand valley-fill deposits in the Upper Cretaceous (Cenomanian) Woodbine Group, East Texas field: regional and local perspectives. *AAPG Bulletin*, 93, 231–269.

Benton, M. J. & Clark, J. M. (1988). Archosaur phylogeny and the relationships of the Crocodylia. In M. J. Benton (Ed.), The *Phylogeny and Classification of the Tetrapods Volume 1*: Amphibians, Reptiles, Birds (pp. 295–338). Clarendon Press, Oxford.

Bergquist, H. R. (1949). Geology of the Woodbine Formation of Cooke, Grayson, and Fannin Counties, Texas. 1: 63,360. U. S. Geological Survey. Oil and Gas Investigations Map OM-98.

Blender Foundation, (2002). Blender 3D creation suite version 2.8. Stichting Blender Foundation, Amsterdam, the Netherlands.

Brochu, C. A. (1996). Closure of neurocentral sutures during crocodilian ontogeny: implications for maturity assessment in fossil archosaurs. *Journal of Vertebrate Paleontology*, 16(1), 49–62.

Brochu, C. A. (2001). Crocodylian snouts in space and time: phylogenetic approaches toward adaptive radiation. *American Zoologist*, 41, 564–585.

Brownstein, C. D. (2018). The biogeography and ecology of the Cretaceous non-avian dinosaurs of Appalachia. *Palaeontologia Electronica*, 21(1), 1–56.

Buscalioni, A. D., Piras, P., Vullo, R., Signor, M., & Barber, C. (2011). Early eusuchia crocodylomorpha from the vertebrate-rich Plattenkalk of Pietraroia (Lower Albian, southern Apennines, Italy). *Zool J Linn Soc*, 163, S199-S227.

D'Amore, D. C., Harmon, M., Drumheller, S. K., & Testin, J. J. (2019). Quantitative heterodonty in Crocodylia: assessing size and shape across modern and extinct taxa. *PeerJ*, 7, e6485.

Dodge, C. F. (1952). Stratigraphy of the Woodbine Formation in the Arlington area. *Tarrant County, Texas: Field and Laboratory*, 20(2), 66–78.

Dodge, C. F. (1968). Stratigraphic Nomenclature of the Woodbine Formation Tarrant County, Texas. In C. F. Dodge (Ed.), *Field trip Guidebook, South Central Section, Stratigraphy of the Woodbine Formation, Tarrant County, Texas* (pp. 107–125). Geological Society of America.

Dodge, C. F. (1969). Stratigraphic nomenclature of the Woodbine Formation Tarrant County, Texas. *Texas Journal of Science*, 21, 43–62.

Donovan, A. D., Gardner, R. D., Pramudito, A., Staerker, T. S., Wehner, M., Corbett, M. J., Lundquist, J. J., Romero, A. M., Henry, L. C., & Rotzien, J. R. (2015). Chronostratigraphic relationships of the Woodbine and Eagle Ford Groups across Texas. *GCAGS Journal*, 4, 67–87.

Drumheller, S. K. & Wilberg, E. W. (2020). A synthetic approach for assessing the interplay of form and function in the crocodyliform snout. *Zoological Journal of the Linnean Society*, 188(2), 507–521.

Drumheller, S. K., Adams, T. L., Maddox, H., & Noto, C. R. (2021). Expanded sampling across ontogeny in *Deltasuchus motherali* (Neosuchia, Crocodyliformes) revealing ecomorphological niche partitioning and Appalachian endemism in Cenomanian crocodyliforms. Cambridge University Press.

Emerson, B. L., Emerson, J. H., Akers, R. E., & Akers, T. J. (1994). *Texas Cretaceous ammonites and nautiloids.* Houston Gem & Mineral Society, Houston, Texas, 439 pp.

Fedorov, A., Beichel, R., Kalpathy-Cramer, J., Finet, J., Fillion-Robin, J. C., Pujol, S., Bauer, C., Jennings, D., Fennessy, F., Sonka, M., & Buatti, J. (2012). 3D Slicer as an image computing platform for the Quantitative Imaging Network. Magnetic Resonance Imaging, 30(9), pp. 1323–1341.

Gignac, P. & O'Brien, H. (2016). Suchian feeding success at the interface of ontogeny and macroevolution. *Integrative and Comparative Biology*, 56(3), 449–458.

Gignac, P. M., Santana, S. E., & O'Brien, H. D. (2019). Ontogenetic inertia explains Neosuchian giants: a case study of *Sarcosuchus imperator* (Archosauria: Suchia). *Journal of Morphology*, 280, S65–S66.

Gradstein, F. M., Ogg, J. G., & Smith, A. G. (Eds.). (2004). A Geologic Time Scale 2004. Cambridge University Press, Cambridge, 500 pp.

Hay, O. P. (1930). Second Bibliography and Catalogue of the Fossil Vertebrata of North America, Volume 1. Carnegie Institution of Washington Publication 390, 990 pp.

Head, J. (1998). A new species of basal hadrosaurid (Dinosauria, Ornithischia) from the Cenomanian of Texas. *Journal of Vertebrate Paleontology*, 18, 718–738.

Hedlund, R. W. (1966). Palynology of the Red Branch Member of the Woodbine Formation (Cenomanian), Bryan County, Oklahoma. *Oklahoma Geological Survey Bulletin*, 112, 1-69.

Hentz, T. F., Ambrose, W. A., & Smith, D. C. (2014). Eaglebine play of the southwestern East Texas basin: stratigraphic and depositional framework of the Upper Cretaceous (Cenomanian-Turonian) Woodbine and Eagle Ford Groups. *AAPG Bulletin*, 98, 2551–2580.

Hill, R. V. (2010). Osteoderms of *Simosuchus clarki* (Crocodyliformes: Notosuchia) from the Late Cretaceous of Madagascar. *Journal of Vertebrate Paleontology*, 30, 154–176.

Huxley, T. H. (1875). On *Stagonolepis robertsoni*, and on the evolution of the Crocodilia. *Quarterly Journal of the Geological Society*, 31, 423–438.

Jacobs, L. L. & Winkler, D. A. (1998). Mammals, archosaurs, and the Early to Late Cretaceous transition in north-central Texas. In Y. Tomida, L. J. Flynn, & L. L. Jacobs (Eds.), *Advances in Vertebrate*

Paleontology and Geochronology (pp. 253–280). National Science Museum, Tokyo.

Johnson, R. O. (1974). Lithofacies and depositional environments of the Rush Creek Member of the Woodbine Formation (Gulfian) of North Central Texas, University of Texas, Arlington, 158 pp.

Jouve, S. & Jalil, N. E. (2020). Paleocene resurrection of a crocodylomorph taxon: biotic crises, climatic and sea level fluctuations. *Gondwana Research*, 85, 1–18.

Jouve, S., de Muizon, C., Cespedes-Paz, R., Sossa-Soruco, V., & Knoll, S. (2021). The longirostrine crocodyliforms from Bolivia and their evolution through the Cretaceous-Palaeogene boundary. *Zoological Journal of the Linnean Society*, 192(2), 475–509.

Kennedy, W. J. & Cobban, W. A. (1990). Cenomanian ammonite faunas from the Woodbine Formation and lower part of the Eagle Ford Group, Texas. *Palaeontology*, 33, 75–154.

Konzhukova, E. D. (1954). [New fossil crocodilian from Mongolia] (in Russian). *Trudy Paleontologicheskogo Instituta ANSSSR*, 48, 171-194.

Krumenacker, L. J., Simon, D. J., Scofield, G., & Varricchio, D. J. (2016). Theropod dinosaurs from the Albian-Cenomanian Wayan Formation of eastern Idaho. *Historical Biology*, 29(2), 170–186.

Lee, Y.-N. (1997). Archosaurs from the Woodbine Formation (Cenomanian) in Texas. *Journal of Paleontology*, 71, 1147–1156.

Main D. J., Parris, D. C., Grandstaff, B. G., & Carter, B. (2011). A new lungfish (Dipnoi; Ceratodontidae) from the Cretaceous Woodbine Formation, Arlington Archosaur Site, North Texas. *Texas Journal of Science*, 63, 283–298.

Main D. J., Noto, C. R., & Weishampel, D. B. (2014). Postcranial anatomy of a basal hadrosauroid (Dinosauria: Ornithopoda) from the Cretaceous (Cenomanian) Woodbine Formation of North Central Texas. In D. A. Eberth & D. C. Evans (Eds.), *Hadrosaurs* (pp. 77–95). Bloomington, IN: Indiana University Press.

Markwick, P. J. (1998a). Crocodilian diversity in space and time: the role of climate in paleoecology and its implication for understanding K/T extinctions. *Paleobiology*, 24(4), 470–497.

Markwick, P. J. (1998b). Fossil crocodilians as indicators of Late Cretaceous and Cenozoic climates: implications for using palaeontological data in reconstructing palaeoclimate. Palaeogeography, Palaeoclimatology. *Palaeoecology*, 137(3-4), 205–271.

McIlhenny EA. (1935). The alligator's life history. Boston: Christopher Publishing House.

Montefeltro, F. C., Larsson, H. C. E., de França, M. A. G., & Langer, M. C. (2013). A new neosuchian with Asian affinities from the Jurassic of northeastern Brazil. *Naturwissenschaften*, 100, 835-841.

Mook, C. C. (1934). A new species of *Teleorhinus* from the Benton Shales. *American Museum Novitates*, 702, 1–11.

NextEngine™, Inc. (2008). HD Desktop 3D scanner and ScanStudio™. NextEngine™, Incorporated, Santa Monica, California.

Noto, C. R. (2015). Archosaur Localities in the Woodbine Formation (Cenomanian) of North-Central Texas. In C. R. Noto (Ed.), *Early- and Mid- Cretaceous Archosaur Localities of North-Central Texas, Fieldtrip Guidebook for the 75th Annaul Meeting of the Society of Vertebrate Paleontology, Dallas, Texas* (pp. 38–51).

Noto, C. R., Main, D. J., & Drumheller, S. K. (2012). Feeding traces and paleobiology of a Cretaceous (Cenomanian) Crocodyliform: example from the Woodbine Formation of Texas. *Palaios*, 27, 105–115.

Noto, C. R., Adams, T. L., Drumheller, S. K., & Turner, A. H. (2019). A small enigmatic neosuchian crocodyliform from the Woodbine Formation of Texas. The Anatomical Record: ar.24174

Noto, C. R., D'Amore, D., Drumheller, S., & Adams, T. (2022). A newly recognized theropod assemblage from the Lewisville Formation (Woodbine Group; Cenomanian) and its implications for understanding Late Cretaceous Appalachian terrestrial ecosystems. *PeerJ*, 10, e12782.

Noto, C., Drumheller, S., Adams, T., Adrian, B., Smith, H., Tykoski, R., & Flaig, P. (2023a). Faunal composition, distribution, and paleobiogeography of fossil vertebrates from the Lewisville Formation (Woodbine Group, Cenomanian). 14th Symposium on Mesozoic Terrestrial Ecosystems and Biota. *Anatomical Record*, 306, 203–206. https://doi.org/10.1002/ar.25219

Noto, C., Flaig, P., Contreras, D., Zippi, P., Lorente, M., Andrzejewski, K., & Tykoski, R. (2023b). Deciphering the Woodbine Group (Late Cretaceous; Cenomanian) outcrops of the Dallas-Ft. Worth Metroplex: new data and new horizons. 14th Symposium on Mesozoic Terrestrial Ecosystems and Biota. *Anatomical Record*, 306, 206–208. https://doi.org/10.1002/ar.25219

Oliver, W. B. (1971). Depositional systems in the Woodbine Formation (Upper Cretaceous), northeast Texas. The University of Texas at Austin, Bureau of Economic Geology, Report of Investigations 73, 28 pp.

Osborn, H. F. (1904). *Teleorhinus browni*—A Teleosaur in the Fort Benton. *Bulletin of the American Museum of Natural History*, 20, 239–240.

Owen, R. (1879). Monograph on the fossil Reptilia of the Wealden and Purbeck formations. Supplement IX, Crocodilia (*Goniopholis*, *Brachydectes*, *Nannosuchus*, *Theriosuchus*, and *Nuthetes*). *Palaeontographical Society of London Monograph*, 33, 1–19.

Powell, J. D. (1968). Woodbine-Eagle Ford transition, Tarrant Member. In F. Dodge (Ed.), *Stratigraphy of the Woodbine Formation: Tarrant County, Texas*. *Field Trip Guidebook* (pp. 27–43). Geological Society of America, South Central Section, Denver.

Prieto-Márquez, A., Erickson, G. M., & Ebersole, J. A. (2016). Anatomy and osteohistology of the basal hadrosaurid dinosaur *Eotrachodon* from the uppermost Santonian (Cretaceous) of southern Appalachia. *PeerJ*, 4, e1872.

Revopoint 3D Technologies, Inc. (2014). Revopoint POP2 3D scanner and Revo Scan. Revopoint 3D Technologies, Incorporated, Shenzhen, China.

Ross, C. A. & Magnusson, W. E. (1989). Living Crocodiles. Crocodiles And Alligators., 58–73 pp.

Salas-Gismondi, R., Flynn, J. J., Baby, P., Tejada-Lara, J. V., Wesselingh, F. P., & Antoine, P. O. (2015). A Miocene hyperdiverse crocodylian community reveals peculiar trophic dynamics in proto-Amazonian mega-wetlands. *Proceedings of the Royal Society B: Biological Sciences*, 282(1804), 20142490.

Suarez C. A., Frederickson, J., Cifelli, R. L., Pittman, J. G., Nydam, R. L., Hunt-Foster, R. K., & Morgan, K. (2021). A new vertebrate fauna from the Lower Cretaceous Holly Creek Formation of the Trinity Group, southwest Arkansas, USA. *PeerJ*, 9, e12242. 10.7717/peerj. 12242

Trudel, P. (1994). Stratigraphic sequences and facies architecture of the Woodbine-Eagle Ford interval, Upper Cretaceous, North Central Texas. unpublished Master's thesis, Tarleton State University, 105 pp.

Turner, A. H. (2004). Crocodyliform biogeography during the Cretaceous: evidence of Gondwanan vicariance from biogeographical analysis. *Proc R Soc Lond B Biol Sci*, 271, 2003–2009.

Ullmann, P. V., Varricchio, D. J., & Knell, M. J. (2012). Taphonomy and taxonomy of a vertebrate microsite in the mid-Cretaceous (Albian-Cenomanian) Blackleaf Formation, southwest Montana. *Historical Biology*, 24, 311–328.

Vallabhaneni, S., Olszewski, T. D., Pope, M. C., & Heidari, Z. (2016). Facies and stratigraphic interpretation of the Eaglebine Play in Central Texas. *GCAGS Journal*, 5, 25–46.

Whetstone, K. & Whybrow, P. (1983). A 'cursorial' crocodilian from the Triassic of Lesotho (Basutoland), southern Africa. *Occasional Publications of the Museum of Natural History of the University of Kansas*, 106, 1–37.

Weishampel, D. B., Barrett, P. M., Coria, R. A., Le Loeuff, J., Xing, X., Xijin, Z., Sahni, A., Gomani, E. M. P., & Noto, C. R. (2004). Dinosaur Distribution. In D. B. Weishampel, P. Dodson, & H. Osmólska (Eds.), *The Dinosauria, second edition* (pp. 517–606).

Winkler, D., Jacobs, L., Lee, Y., & Murry, P. (1995). Sea level fluctuation and terrestrial faunal change in North-Central Texas. In A. Sun & Y. Wang (Eds.), *Sixth Symposium on Mesozoic Terrestrial Ecosystems and Biota, Short Papers* (pp. 175–177). China Ocean Press, Beijing.

Wu, X.-C., Russell, A. P., & Cumbaa, S. L. (2001). *Terminonaris* (Archosauria: Crocodyliformes): new material from Saskatchewan, Canada, and comments on its phylogenetic relationships. *Journal of Vertebrate Paleontology*, 21, 492–514.

Zanno, L. E. & Makovicky, P. J. (2011). On the earliest record of Cretaceous tyrannosauroids in western North America: implications for an Early Cretaceous Laurasian interchange event. *Historical Biology*, 23, 317–325. 10.1080/08912963.2010.543952

Zanno, L. E. & Makovicky, P. J. (2013). Neovenatorid theropods are apex predators in the Late Cretaceous of North America. *Nature Communications*, 4, 2827.

Zittel, K. A. & Eastman, C. R. (1902). *Text Book of Palaeontology.* Macmillan and Co., London, 283 pp.

APPENDIX 1. Cranial

Specimen #	Element	Max Length	Max Width	Max Height	Taxa
2013-07-0018a	Maxilla	55.21	29.25	10.46	Crocodyliform indet.
2013-07-0018b	Palate	75.05	40.80	9.64	Crocodyliform indet.
2013-07-1066	Dentary	12.46	4.56	4.9	eusuchian indet.
2013-07-2085	Dentary	17.83	6.53	5.6	eusuchian indet.
2013-07-0171	Tooth	37.61	15.69		Terminonaris sp.
2013-07-0168	Tooth	38.01	15.29		Terminonaris sp.

APPENDIX 2. Alveoli diameters

Specimen #	Alveolus position	Length (mm)	*measured anteroposteriorly*
2013-07-0018a	M-1	4.53	
	M-2	4.47	
	M-3	6.22	
	M-4	3.81	
	M-5	4.36	
	M-6	3.8	
	M-7	4.04	
	M-8	4.49	
2013-07-0018b	M-a	3.84	
	M-b	4.25	
	M-c	3.32	
	M-d	2.8	

APPENDIX 3. Vertebrae

Specimen #	Element	Max Length	Max Width	Max Height	Notes
2013-07-1779	Cervical	9.61	8.01	7.28	
2013-07-0537	Dorsal	14.36	8.09	6.46	height of neural arch 13.71
2013-07-0713	Dorsal	21.22	12.31	11.65	
2013-07-0714	Dorsal	13.45	7.55	6.86	
2013-07-0718	Dorsal	12.35	7.72	7.23	
2013-07-2064	Dorsal	15.05	7.53	8.35	
2013-07-2066	Dorsal	14.05	9.63	10.03	deep ventral keel
2013-07-2073	Dorsal	18.53	10.27	8.71	
2013-07-0056	Caudal	16.29	7.94	7.75	
2013-07-0715	Caudal	30.10	16.12	13.51	
2013-07-0716	Caudal	12.10	5.02	12.38	height of centrum 4.68
2013-07-1665	Caudal	11.05	6.68	5.73	
2013-07-2068	Caudal	13.24	6.04	8.07	
2013-07-2069	Caudal	11.07	3.16	6.76	

APPENDIX 4. Osteoderms

Specimen #	Morphotype	AP Length	ML Width	AM length	Depth	W/L ratio	AM/AP	Notes
2013-07-1269	1	19.57	16.35	7.48	5.34	0.84	0.38	
2013-07-1270	1	18.96	16.21	8.53	3.31	0.85	0.45	
2013-07-1272	1	16.63	13.15	6.36	2.69	0.79	0.38	
2013-07-1273	1	24.32	21.95	9.70	2.71	0.90	0.40	
2013-07-1274	1	27.23	21.02	9.98	3.36	0.77	0.37	
2013-07-1276	1	20.18	15.04	9.98	2.59	0.75	0.49	
2013-07-1277	1	19.61	16.45	8.39	4.59	0.84	0.43	
2013-07-1280	1	19.09	14.72	8.29	3.70	0.77	0.43	
2013-07-1283	1	24.77		10.45	3.35	0.00	0.42	Fragmentary
2013-07-1662	1	21.93	16.45	9.91	3.16	0.75	0.45	
2013-07-1946	1	19.61	19.37	7.38	3.29	0.99	0.38	
2013-07-2079	1	16.64	15.80	6.12	1.92	0.95	0.37	
2013-07-2083	1	16.77	16.24	7.18	2.60	0.97	0.43	
2013-07-2086	1	25.28	20.93	9.51	2.72	0.83	0.38	
2013-07-2087	1	26.98	20.57	11.47	4.60	0.76	0.43	
2013-07-0035	2	20.77	28.52		2.91	1.37		
2013-07-1271	2	7.62	10.41		1.97	1.37		
2013-07-1281	2	17.11	18.73		4.20	1.09		
2013-07-1439	2	9.22	14.13		1.76	1.53		
2013-07-1474	2	30.94	30.94		4.98	1.00		
2013-07-1509	2	9.31	13.67		1.79	1.47		Fragmentary
2013-07-2057	2	12.07	11.12		1.36	0.92		Fragmentary
2013-07-2065	2	19.10	22.48		3.15	1.18		shallow keel
2013-07-2074	2	8.10	12.31		1.09	1.52		shallow keel
2013-07-2075	2	10.64	12.56		1.46	1.18		Fragmentary
2013-07-2076	2	14.28	19.92		1.74	1.39		
2013-07-2077	2	14.80	15.05		1.42	1.02		strongly concave
2013-07-2080	2	15.72	18.94		2.00	1.20		
2013-07-0020	3	27.26	19.71		4.25	0.72		keel; concave
2013-07-1477	3	17.27	18.03		2.04	1.04		keel; concave
2013-07-1539	3	17.39	11.68		2.09	0.67		keel; concave; Fragmentary
2013-07-2067	3	21.00	18.91		2.57	0.90		keel; concave
2013-07-2072	3	13.19	6.89		1.09	0.52		keel; concave; Fragmentary
2013-07-2078	3	20.87	14.91		2.87	0.71		keel; concave
2013-07-2081	3	19.18	14.86		2.00	0.77		keel; concave
2013-07-2082	3	20.32	16.21		2.30	0.80		keel; concave
2013-07-1065	4	10.29	5.48		0.98	0.53		keel; concave
2013-07-2071	4	12.03	7.39		1.20	0.61		keel; concave
2013-07-0037		16.45	24.09		2.00	1.46		no keel; no art. Margin
2013-07-1562		32.74	36.28		6.91	1.11		strongly concave; keel; rounded edge